Electronic Supplementary Material (ESI) for ChemComm.

Supporting Information

Contemporaneous Oxidation State Manipulation to Accelerate Intermediates Desorption for Overall Water Electrolysis

Yongqiang Zhao[a], Bo Jin[a], Anthony Vasileff[a], Yan Jiao[a], Shi-Zhang Qiao*[a]

[a] School of Chemical Engineering, The University of Adelaide, Adelaide, SA 5005, Australia

E-mail: s.qiao@adelaide.edu.au

Experimental

Chemicals: Hydrochloric acid (ACS reagent, 37%) and thiourea (≥99.0%) were purchased from Sigma-Aldrich and used without further purification. Milli-Q water (18.2 M Ωcm, PURELAB Option-Q) was used in all experiments. The cobalt foil (99.95% trace metals basis, thickness 0.01 cm) was washed with dilute HCl, ultrapure water, acetone, and ethanol, and then dried under vacuum at 25 °C before use.

Fabrication of activated cobalt oxide hydroxide (ACo): A pre-cleaned piece of cobalt foil (1.5 cm × 0.3 cm × 0.01 cm, length × width × height) and 10 mL of 3 M HCl were sealed in a reagent bottle and then heated at 140 °C for 1 h. The cobalt foil was then taken out and washed with water to obtain ACo.

Fabrication of cobalt nitride and sulfide (CoNS): The CoNS electrode was fabricated by a one-step calcination of ACo with thiourea in a vacuum sealed ampoule. In a typical synthesis, a piece of ACo and thiourea were sealed in an ampoule under vacuum and then calcinated at 550 °C for 5 h. The heating rate was 5 °C min^{-1} and the cooling process took place naturally. A variety of ACo to thiourea mass ratios, i.e., 1:0.05, 1:0.09, 1:0.14, 1:0.21, and 1:0.35, were employed. In the order of smallest to largest ACo : thiourea mass ratio, the as-prepared cobalt nitride and sulfide electrodes were denoted CoNS1, CoNS2, CoNS3, CoNS4, and CoNS5, respectively. In a typical synthesis, a piece of ACo (32.97 mg) is used to synthesize CoNS3. The calculated Co_2N is 14.02 mg and Co_9S_8 is 3.71 mg. Similarly, a piece of ACo (38.32 mg) is used to synthesize CoNS2. The calculated Co_2N is 5.80 mg and Co_9S_8 is 5.88 mg. The CoNS electrodes were washed with ethanol and water and dried under vacuum at 25 °C before use.

Fabrication of Pt-C and Ir-C Loaded Electrodes: 4 mg of Pt-C or Ir-C were dispersed in 1 mL of water followed by sonication for 30 min to obtain a homogeneous catalyst ink. 150 μL of the catalyst ink and 40 μL 2% Nafion solution were loaded in succession on the surface of Ni foam (surface area: 0.6 cm^2). The overall loading amount was 1 mg cm^{-2}.

Electrochemical Characterization: OER and HER measurements were performed on a CHI 760D Bipotentiostat (CH Instruments, Inc., USA) in O_2 or Ar saturated 1.0 M KOH aqueous solution using a conventional three-electrode system with a graphite rod as the counter electrode and Ag/AgCl (4 M KCl) as the reference electrode. Overall water splitting measurements were performed in a three-electrode glass cell. The current density was normalized to the geometric surface area and the measured potentials versus Ag/AgCl were converted to the reversible hydrogen electrode (RHE) scale according to the Nernst equation:

$$E_{RHE} = E_{Ag/AgCl} + 0.059 \times pH + 0.205 \quad (1)$$

The polarization curves were recorded in the range of 1.0-1.8 V vs. RHE for the OER and -0.6 to 0 V vs. RHE for the HER at a slow scan rate of 5 mV s^{-1} to minimize the capacitive current. The working electrodes were scanned several times until the signals stabilized, and then the data for polarization curves were collected and corrected for the iR contribution within the cell. The stability test was conducted using a controlled-potential electrolysis method without iR compensation. The EIS was obtained by AC impedance spectroscopy within the frequency range from 0.01 to 100 kHz in 1.0 M KOH. The equivalent circuit for fitting of the EIS data was achieved with ZView software. The Tafel slope was calculated according to Tafel equation as follows:

$$\eta = b\log(j/j_0) \quad (2)$$

where η denotes the overpotential, b denotes the Tafel slope, j denotes the current density, and j_0 denotes the exchange current density. The onset potentials were determined based on the beginning of the linear region in the Tafel plots. The overpotential was calculated as follows:

$$\eta = E\ (\text{vs RHE}) - Er\ (\text{vs RHE}) \quad (3)$$

where E denotes the actual applied potential and Er denotes the reversible potential of the reaction. *E*r is 1.23 V versus RHE for the OER and 0 V vs. RHE for the HER. HER η is always negative. The electrochemical surface area of the electrodes was related to double layer charging curves using cyclic voltammetry in the potential range 0.606 - 0.656 V (vs. RHE) for CoNS3 and ACo, 0.611 - 0.561 V (vs. RHE) for CoNS2 and ACo. The double-layer capacitance values were determined from the slope of the capacitive current versus the scan rate.

Physicochemical Characterization: The scanning transmission electron microscopy (STEM) images and corresponding mapping images were obtained on a FEI Titan Themis 80-200 system. Transmission electron microscopy (TEM) images and the selected area electron diffraction (SAED) patterns were obtained on a JEOL 2100F microscope at an acceleration voltage of 200 kV. Scanning electron microscopy (SEM) images and energy dispersive spectra (EDS) were collected on a FEI Quanta 450 at high vacuum with an accelerating voltage of 20 kV. X-ray diffraction (XRD) patterns were collected on a powder X-ray diffractometer at 40 kV and 15 mA using Co-Kα radiation (Miniflex, Rigaku). X-ray photoelectron spectra (XPS) were obtained using an Axis Ultra (Kratos Analytical, UK) XPS spectrometer equipped with an Al Kα source (1486.6 eV).

Supplementary Results

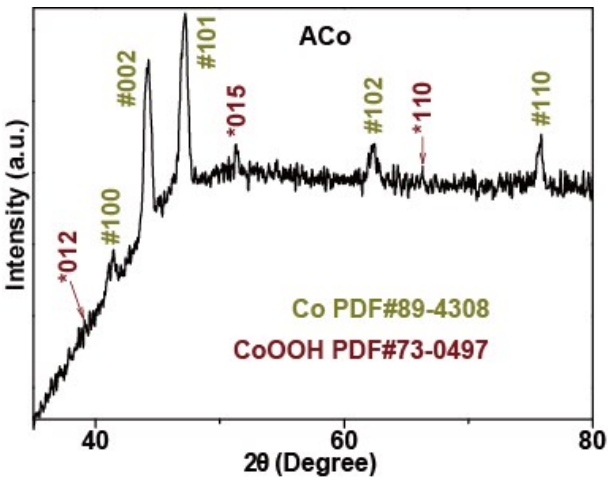

Fig. S1 XRD pattern of ACo.

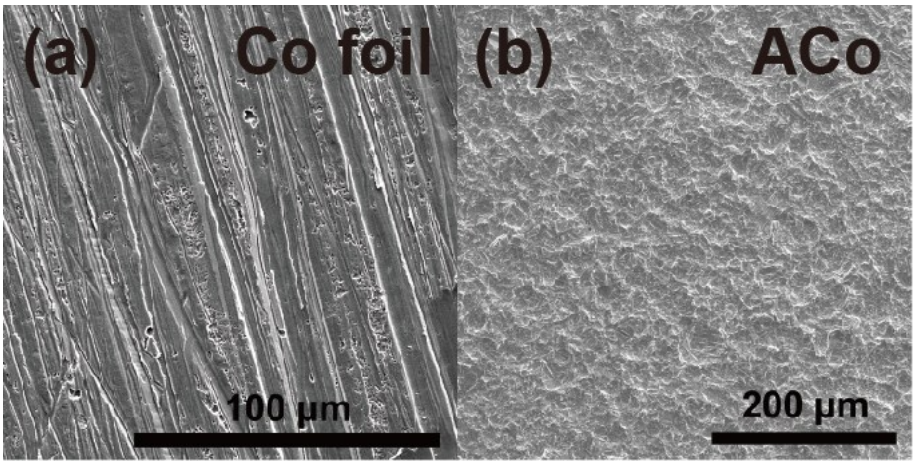

Fig. S2 SEM image of (a) cobalt foil and (b) ACo.

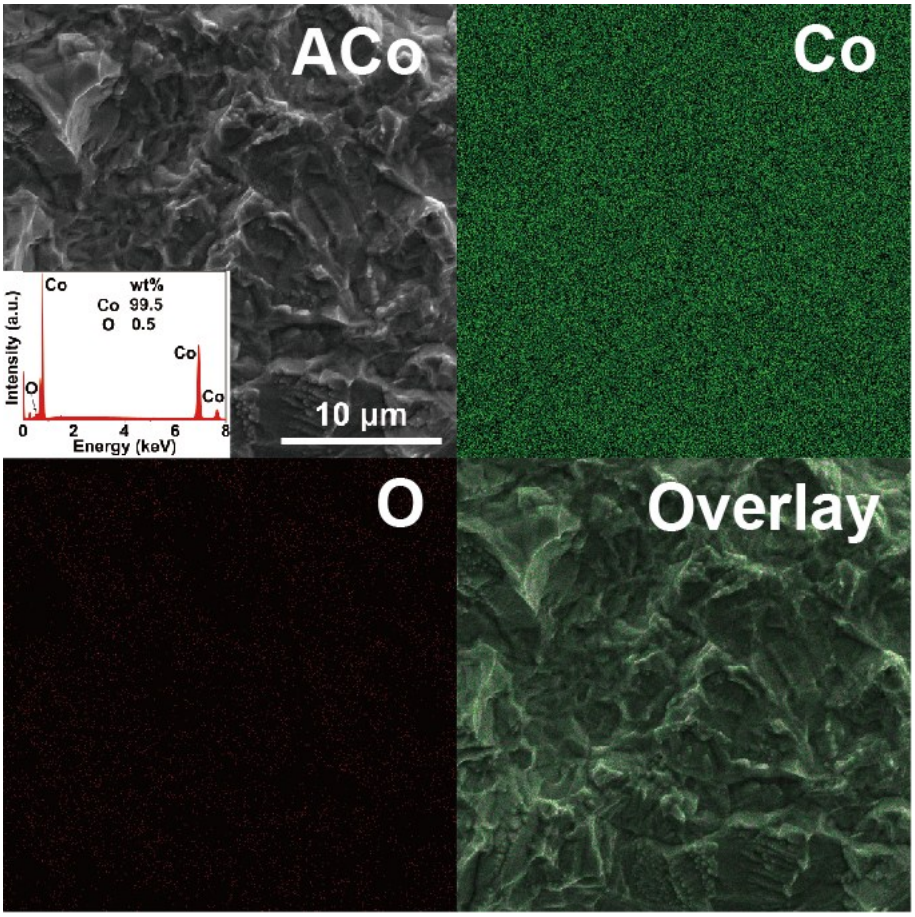

Fig. S3 SEM image and (inset) EDS spectra of ACo and corresponding mapping of cobalt, oxygen and overlay.

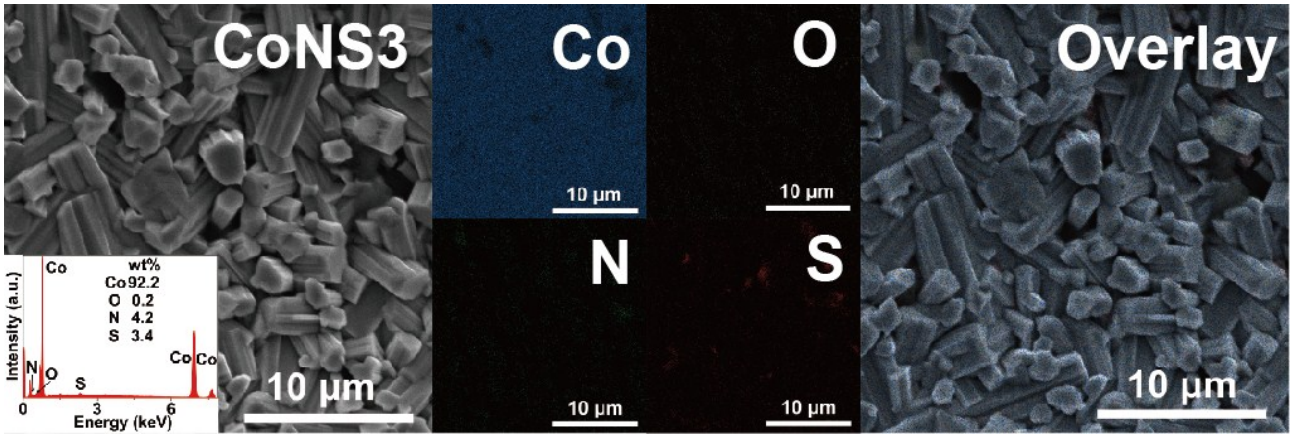

Fig. S4 SEM image and (inset) EDS spectra of CoNS3 and corresponding mapping of cobalt, oxygen, nitrogen, sulfur, and overlay.

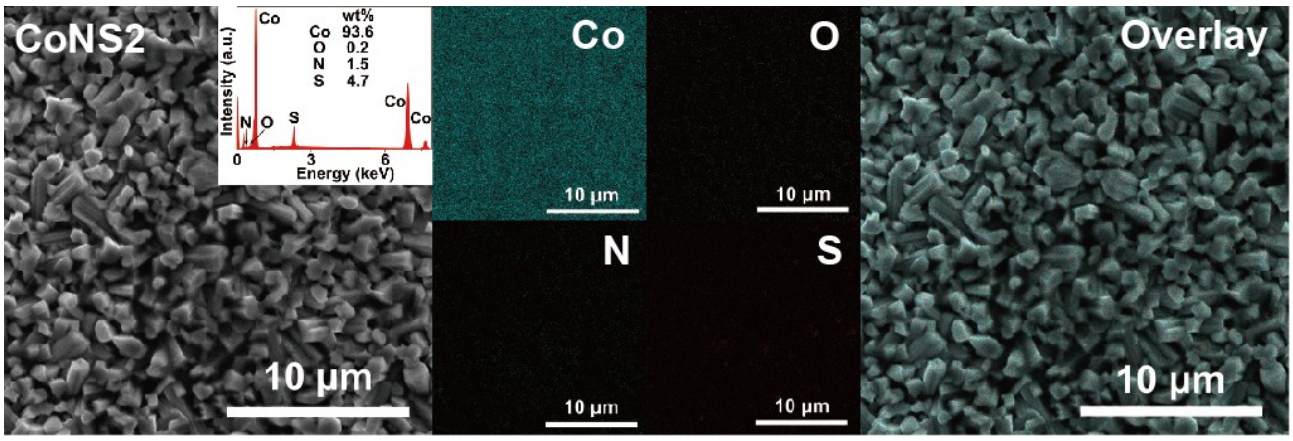

Fig. S5 SEM image and (inset) EDS spectra of CoNS2 and corresponding mapping of cobalt, oxygen, nitrogen, sulfur, and overlay.

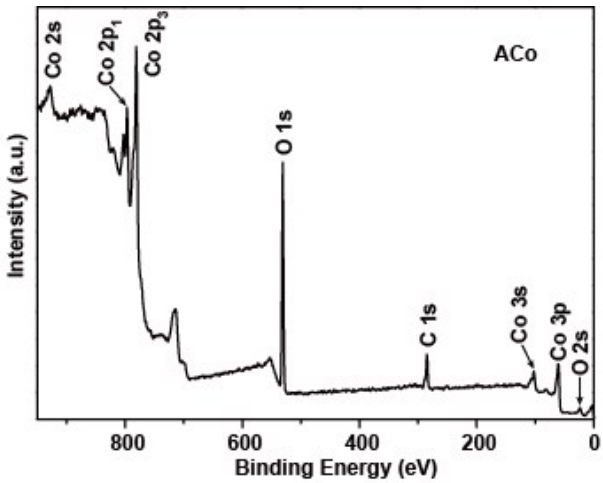

Fig. S6 XPS survey spectrum of ACo.

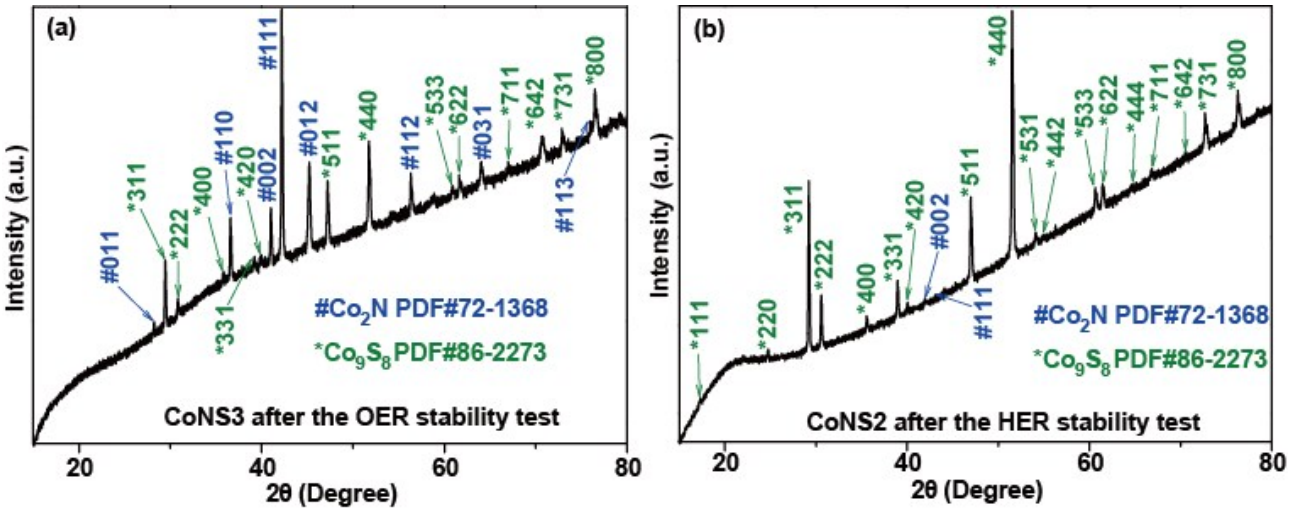

Fig. S7 XRD patterns of (a) CoNS3 and (b) CoNS2 after cycle stability tests.

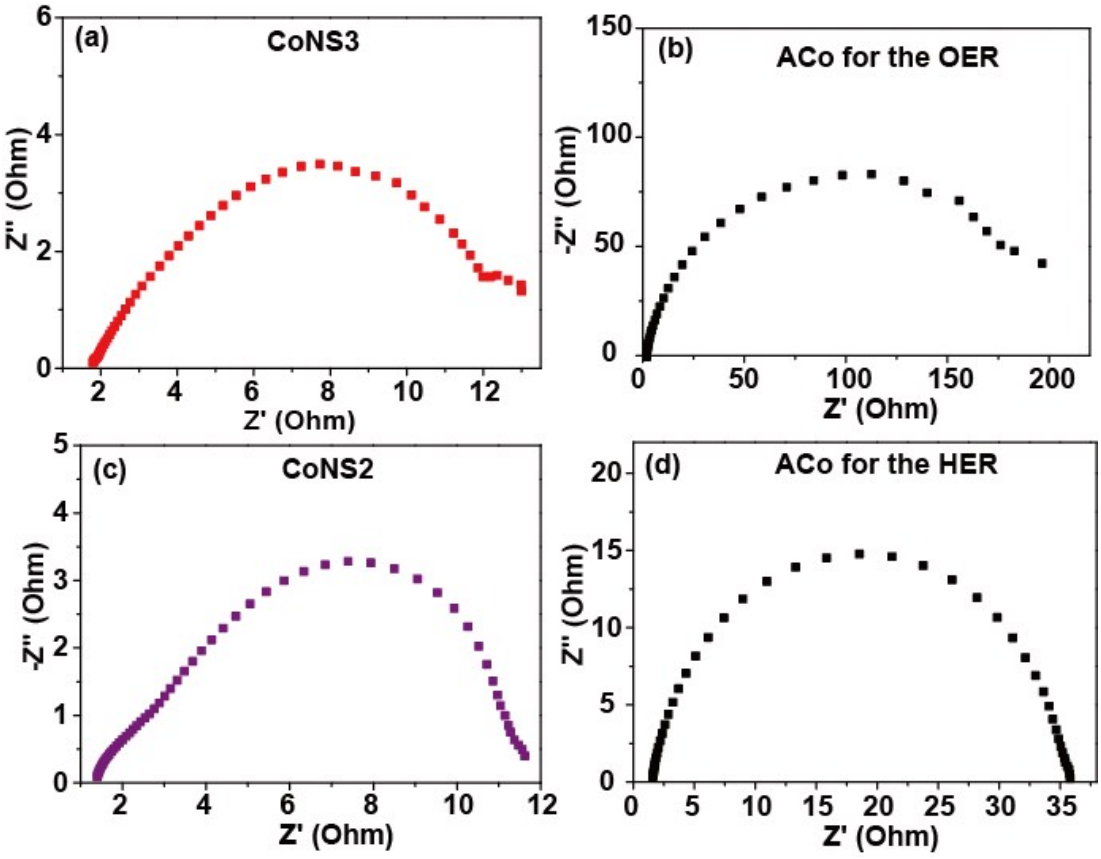

Fig. S8 Nyquist plots of (a) CoNS3, (b) ACo for the OER process in 1.0 M KOH at a potential of 1.42 V (vs. RHE) and (c) CoNS2, (d) ACo for the HER process in 1.0 M KOH at a potential of -0.319 V (vs. RHE).

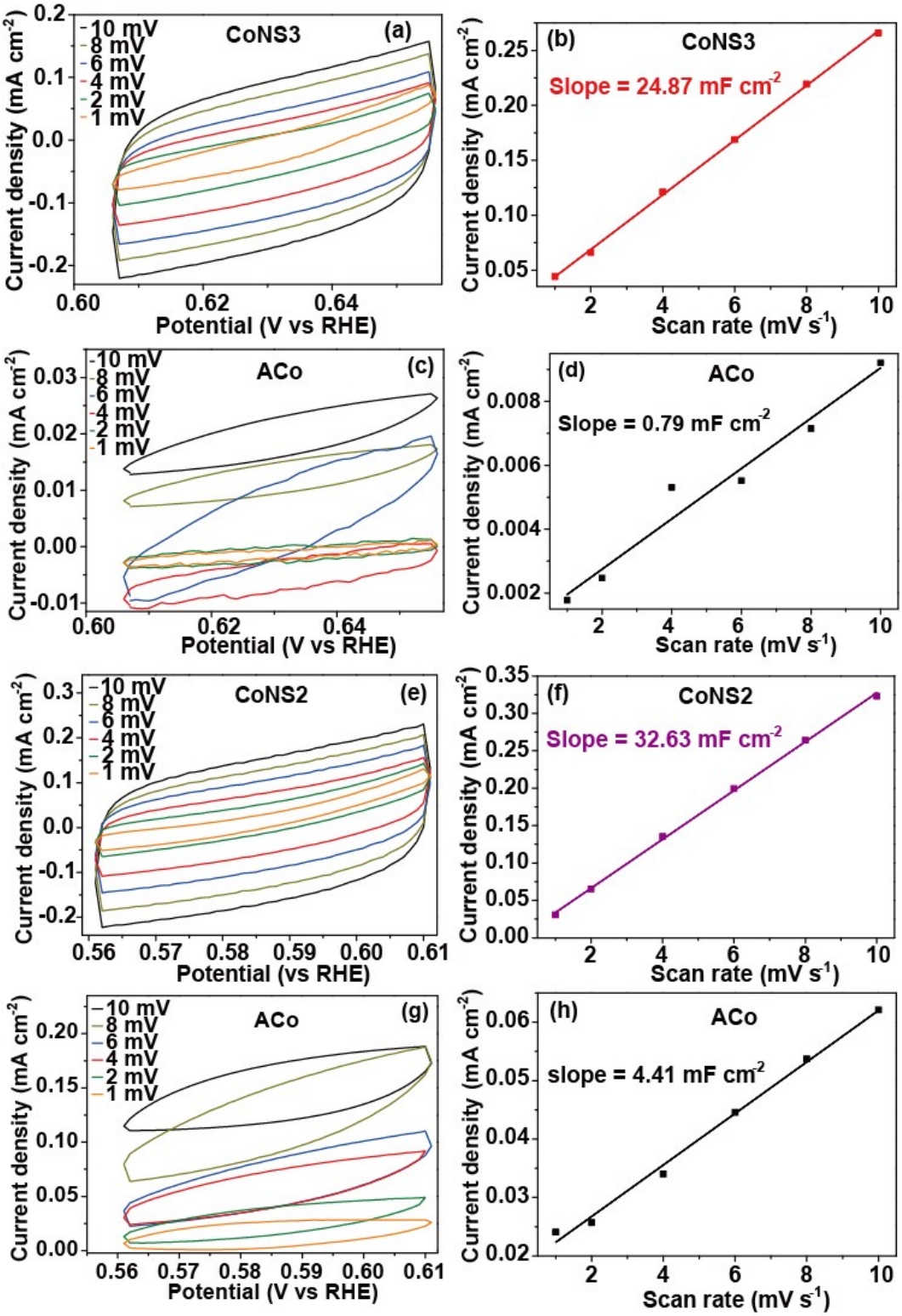

Fig. S9 The double-layer region with scan rates ranging from 1 to 10 mV s^{-1} in 1.0 M KOH for (a) CoNS3 and (c) ACo in 0.606 - 0.656 V (vs. RHE), (e) CoNS2 and (g) ACo in 0.611 - 0.561 V (vs. RHE). Charging current density with different scan rates for (b) CoNS3 and (d) ACo in 0.606 - 0.656 V (vs. RHE), (f) CoNS2 and (h) ACo in 0.611 - 0.561 V (vs. RHE).

Table S1 OER performance comparison between CoNS3 and recently reported electrocatalysts in alkaline media

Electrocatalysts	Electrolyte	j, mA cm^{-2}	η required, mV	Tafel slop, mV dec^{-1}	Reference
CoNS3	1.0 M KOH	100	275	109.1	This work
MoS_2/NiS NCs	1.0 M KOH	100	~475	53	S1
NCP/G NSs	1.0 M KOH	100	400	65.9	S2
NF@Ni/C-600	1.0 M KOH	100	~460	54	S3
Ni_3S_2/NF-2	1.0 M KOH	100	425	N/A	S4
Fe_1-$(Co_3O_4)_{10}$ holy nanosheets	1.0 M KOH	100	~410	55	S5
$NiCo_2O_4$@$CoMoO_4$/NF-7	1.0 M KOH	100	~510	102	S6
Ni-Mo_xC/NC-100	1.0 M KOH	100	470	74	S7
NiSe-$Ni_{0.85}Se$/CP	1.0 M KOH	100	420	75	S8
NiMoN-NF700	1.0 M KOH	100	~405	54	S9
$NiCo_2O_4$ nanowire arrays	1.0 M KOH	100	470	66.9	S10

Table S2 HER performance comparison between CoNS2 and recently reported electrocatalysts in alkaline media

Electrocatalysts	Electrolyte	j, mA cm^{-2}	η required, mV	Tafel slop, mV dec^{-1}	Reference
CoNS2	1.0 M KOH	100	335	141.1	This work
Ni:Co_3S_4	1.0 M KOH	100	330	91	S11
np-$Co_9S_{7.1}P_{0.9}$	1.0 M KOH	100	320	102	S12
NFNS@NiP@Truss	1.0 M KOH	100	380	141	S13
$Ni_{0.75}Co_{0.25}P$/NC	1.0 M KOH	100	360	122	S14
$Ni_3(S_{0.25}Se_{0.75})_2$@NiOOH	1.0 M KOH	100	400	87	S15
Ni_1Co_1P NWs	1.0 M KOH	100	397	102.1	S16
$Ni_{1-x}Fe_x$-LDH	1.0 M KOH	100	380	110	S17
NC@CoN_x/CF	1.0 M KOH	100	380	128	S18
Zn-Co-S/TM	1.0 M KOH	100	382	164	S19
Ni_3N nanosheets on carbon cloth	1.0 M KOH	100	470	N/A	S20

Reference

1. Z. Zhai, C. Li, L. Zhang, H.-C. Wu, L. Zhang, N. Tang, W. Wang and J. Gong, *J. Mater. Chem. A*, 2018, **6**, 9833-9838.
2. J. Tian, J. Chen, J. Liu, Q. Tian and P. Chen, *Nano Energy*, 2018, **48**, 284-291.
3. H. Sun, Y. Lian, C. Yang, L. Xiong, P. Qi, Q. Mu, X. Zhao, J. Guo, Z. Deng and Y. Peng, *Energy. Environ. Sci.*, 2018, **11**, 2363-2371.
4. G. Liu, Z. Sun, X. Zhang, H. Wang, G. Wang, X. Wu, H. Zhang and H. Zhao, *J. Mater. Chem. A*, 2018, **6**, 19201-19209.
5. Y. Li, F.-M. Li, X.-Y. Meng, X.-R. Wu, S.-N. Li and Y. Chen, *Nano Energy*, 2018, **54**, 238-250.
6. Y. Gong, Z. Yang, Y. Lin, J. Wang, H. Pan and Z. Xu, *J. Mater. Chem. A*, 2018, **6**, 16950-16958.
7. D. Das, S. Santra and K. K. Nanda, *ACS Appl. Mater. Interfaces*, 2018, **10**, 35025-35038.
8. Y. Chen, Z. Ren, H. Fu, X. Zhang, G. Tian and H. Fu, *Small*, 2018, **14**, 1800763.
9. B. Chang, J. Yang, Y. Shao, L. Zhang, W. Fan, B. Huang, Y. Wu and X. Hao, *ChemSusChem*, 2018, **11**, 3198-3207.
10. A. Sivanantham, P. Ganesan and S. Shanmugam, *Adv. Funct. Mater.*, 2016, **26**, 4661-4672.
11. S. Tang, X. Wang, Y. Zhang, M. Courté, H. J. Fan and D. Fichou, *Nanoscale*, 2019, **11**, 2202-2210.
12. Y. Tan, M. Luo, P. Liu, C. Cheng, J. Han, K. Watanabe and M. Chen, *ACS Appl. Mater. Interfaces*, 2019, **11**, 3880-3888.
13. X. Su, X. Li, C. Y. A. Ong, T. S. Herng, Y. Wang, E. Peng and J. Ding, *Advanced Science*, 2019, **6**, 1801670.
14. R. Boppella, J. Tan, W. Yang and J. Moon, *Adv. Funct. Mater.*, 2019, **29**, 1807976.
15. X. Zheng, Y. Zhang, H. Liu, D. Fu, J. Chen, J. Wang, C. Zhong, Y. Deng, X. Han and W. Hu, *Small*, 2018, **14**, 1803666.
16. H. Xu, J. Wei, M. Zhang, J. Wang, Y. Shiraishi, L. Tian and Y. Du, *Nanoscale*, 2018, **10**, 18767-18773.
17. G. Rajeshkhanna, T. I. Singh, N. H. Kim and J. H. Lee, *ACS Appl. Mater. Interfaces*, 2018, **10**, 42453-42468.

18. J. Zheng, X. Chen, X. Zhong, S. Li, T. Liu, G. Zhuang, X. Li, S. Deng, D. Mei and J.-G. Wang, *Adv. Funct. Mater.*, 2017, **27**, 1704169.

19. Y. Liang, Q. Liu, Y. Luo, X. Sun, Y. He and A. M. Asiri, *Electrochim. Acta*, 2016, **190**, 360-364.

20. D. Gao, J. Zhang, T. Wang, W. Xiao, K. Tao, D. Xue and J. Ding, *J. Mater. Chem. A*, 2016, **4**, 17363-17369.